Passive Homing Missile Guidance Law Based on New Target Maneuver Models

Jason L. Speyer* and Kevin D. Kim†
University of Texas at Austin, Austin, Texas 78703
and
Minjea Tahk‡
Korea Advanced Institute of Science and Technology, Seoul, Korea

A new stochastic dynamic target model is proposed on the assumption that certain targets execute evasive maneuvers orthogonal to their velocity vector. Along with this new acceleration dynamic model, the orthogonality is also enforced by the addition of a fictitious auxiliary measurement. The target states are estimated by the modified-gain extended Kalman filter, and the angular target maneuver rate is constructed online. A guidance law that minimizes a quadratic performance index subject to the assumed stochastic engagement dynamics that includes state-dependent noise is derived. This guidance law is determined in closed form where the gains are an explicit function of the estimated target maneuver rate as well as time to go. The numerical simulation for the two-dimensional angle-only measurement case indicates that the proposed target model leads to significant improvement in the estimation of the target states. Furthermore, the effect on terminal miss distance using this new guidance scheme is given and compared to the Gauss-Markov model.

I. Introduction

THE target-tracking problem for homing missile guidance involves the problem of estimating large and rapidly changing target accelerations. The time history of target motion is inherently a jump process whereby the acceleration levels and switching times are unkown a priori. Because of this arbitrary and unpredictable nature of target maneuverability, target acceleration cannot easily be modeled.

A considerable number of tracking methods for maneuvering targets have been proposed and developed for both new target models and filtering techniques.[1-8] In spite of the numerous modeling and filtering techniques available, target acceleration estimation using angle-only measurements is relatively poor. Usually, the target-tracking problem is approached by modeling target acceleration with a first-order Gauss-Markov model and applying the extended Kalman filter (EKF). One difficulty with the Gauss-Markov model is that the assumed large-process noise spectral density induces Kalman filter divergence even when the target maneuver is not present and can lead to a target acceleration magnitude estimate that exceeds the actual maximum. Another problem is that the target motion is not well-represented by the Gauss-Markov diffusion process.

In an effort to alleviate these problems, the circular target model has been proposed as a target motion model, where the phase angle is a Brownian motion process and the acceleration magnitude can be either a random variable or a bounded stochastic process. This target model was suggested in Ref. 4 using concepts extracted from Refs. 9 and 10.

By including a priori knowledge of the target motion, improved estimates of the target states can be obtained. This idea is included in Refs. 6 and 7 by using a target acceleration model that employs a target mean jerk term. For conventional targets such as winged aircraft, the longitudinal acceleration component is often negligible compared to the lateral component in evasive maneuvers. This notion fits the circular target model in which the angular rate term is estimated to account for the actual dynamics of the coordinated turn. This model is presented in Sec. II. However, an approximate state expansion is required to handle the unknown angular rate in the target model. This approximate dynamical system used for estimation is presented in Secs. III.A and III.B. Furthermore, in Sec. III.C the orthogonality between target velocity and acceleration can be viewed as a kinematic constraint where compliance is enforced by including this constraint as a pseudomeasurement.[7,8] The approximate target dynamics and pseudomeasurement are included in the modified-gain extended Kalman filter (MGEKF)[11] and are presented in Sec. IV. The MGEKF is selected because of its superior performance over the EKF especially for bearing-only problems. In Sec. V, a linear quadratic guidance law is derived for this circular target model. This guidance law remains a linear function of the estimated states, but the guidance gains obtained in closed form are a nonlinear function of the estimated rotation rate and time to go. Finally, a numerical simulation is performed for a two-dimensional homing missile intercept problem. Both the estimation process and the terminal miss are enhanced by the new models and the associated estimator and guidance law in comparison with the Gauss-Markov model.

II. Target Acceleration Model

In this section, the circular target acceleration model is presented, and the dynamic consistency between this target model and an assumed nonlinear target model is discussed.

A. Circular Target Motion

The two-dimensional homing missile guidance scenario is described by two sets of nonlinear dynamic equations of mo-

Received June 15, 1989; revision received Jan. 30, 1990; presented as Paper 90-3378 at the AIAA Guidance, Navigation, and Control Conference, Portland, OR, Aug. 20-22, 1990.

*Harry H. Power Professor; currently, Professor, Mechanical, Aerospace, and Nuclear Engineering Department, University of California, Los Angeles. Fellow AIAA.

†Graduate Research Assistant. Student Member AIAA.

‡Assistant Professor, Department of Mechanical Engineering. Member AIAA.

tion for the missile and target

$$\dot{x}_M = V_M \cos\theta_M, \qquad \dot{x}_T = V_T \cos\theta_T$$
$$\dot{y}_M = V_M \sin\theta_M, \qquad \dot{y}_T = V_T \sin\theta_T$$
$$\dot{V}_M = a_{M_t}, \qquad \dot{V}_T = 0$$
$$\dot{\theta}_M = a_{M_n}/V_M, \qquad \dot{\theta}_T = a_T/V_T \tag{1}$$

where (x_M, x_T) and (y_M, y_T) are inertial coordinates, V_M and V_T are the velocities, a_{M_t}, a_{M_n}, and a_T are the accelerations, and θ_M and θ_T are the flight-path angles (Fig. 1). The subscripts M and T denote the missile and target, respectively, and a_{M_t} and a_{M_n} are tangential and normal accelerations, respectively. Only the normal component of the acceleration contributes to changing the angular orientations of each vehicle, and the target is assumed to fly at constant speed.

The following target model is assumed to be used in the filter. The objective is to choose a model that is linear in order to reduce the numerical computation of the filter, but reasonably consistent with the nonlinear model so that the estimates are of good quality. The target model for the filter in two dimensions is

$$a_{T_x}(t) = a_T \cos(\omega t + \theta), \qquad a_{T_y}(t) = a_T \sin(\omega t + \theta) \tag{2}$$

where a_T is a constant that is unknown a priori, ω is the angular velocity to be estimated in a right-handed coordinate system, and θ is a Brownian motion process to represent a random target maneuver phase with statistics

$$E[\mathrm{d}\theta] = 0, \qquad E[\mathrm{d}\theta^2] = \Theta \mathrm{d}t, \qquad \Theta = 1/\tau_\Theta \tag{3}$$

where $E[\cdot]$ denotes the expectation operator. Here, Θ is the power spectral density of the process and τ_Θ is the coherence time, the time for the standard deviation of θ to reach 1 rad. Whereas in the previous circular target model[4] the acceleration components were just a diffusion process along a circle, those in the new model are related to the actual target motion through a term of physical meaning, ω.

B. Dynamic Consistency

To see how the current model approximates the assumed nonlinear target dynamics Eq. (1), consider a deterministically equivalent case. The integration of Eq. (2) with $\theta = 0$ and $|\omega| > 0$ yields

$$V_x = \frac{a_T}{\omega}\sin\omega t, \qquad V_y = -\frac{a_T}{\omega}\cos\omega t - V_T + \frac{a_T}{\omega} \tag{4}$$

where the initial conditions are $V_x = 0$ and $V_y = -V_T$. Adding the square of each component and moving all terms to the left-hand side gives

$$2(1-\cos\omega t)\left[\left(\frac{a_T}{\omega}\right)^2 - \frac{a_T}{\omega}V_T\right] = 0 \tag{5}$$

For this equation to hold for all $t \geq 0$,

$$\omega = a_T/V_T \tag{6}$$

which is equivalent to the differential equation for the angular rate in Eq. (1).

Furthermore, by taking the dot product of the velocity vector with the acceleration vector, we obtain

$$V_T \cdot a_T = a_T\left[-V_T + (a_T/\omega)\right]\sin\omega t = 0 \tag{7}$$

using Eq. (6) for all $t \geq 0$. This orthogonality between target velocity and acceleration demonstrates the dynamic consistency of the proposed target acceleration model for the filter with the nonlinear target dynamics.

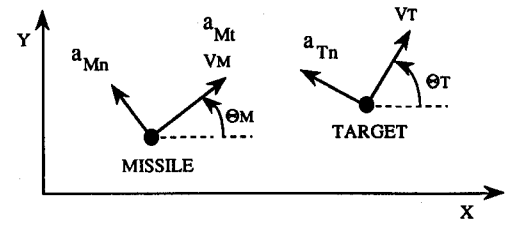

Fig. 1 Inertial reference frame for missile and target.

III. New Dynamic and Measurement Models for Estimation

The previous section dealt with a new circular model for filter implementation in order to exploit an assumed characterization of the motion of a typical target. In this section, the stochastic dynamic equations for the new target model are derived. Furthermore, the kinematic fictitious measurement suggested in Refs. 7 and 8 is also discussed.

A. Formulation and Approximation

Itô stochastic calculus[12] applied to Eq. (2) results in a stochastic differential equation with white state-dependent noise[9]

$$\begin{bmatrix} \mathrm{d}a_{T_x} \\ \mathrm{d}a_{T_y} \end{bmatrix} = \begin{bmatrix} -\Theta/2 & -\omega \\ \omega & -\Theta/2 \end{bmatrix}\begin{bmatrix} a_{T_x} \\ a_{T_y} \end{bmatrix}\mathrm{d}t + \begin{bmatrix} 0 & -\mathrm{d}\theta \\ \mathrm{d}\theta & 0 \end{bmatrix}\begin{bmatrix} a_{T_x} \\ a_{T_y} \end{bmatrix} \tag{8}$$

where the elements $-(\Theta/2)$ in the drift coefficient are the Itô correction terms. Note that the problem is nonlinear due to the unknown ω. To avoid solving the nonlinear problem, ω is approximately removed by an expansion of state variables as in Ref. 10. Define new states as

$$a_x^1 = \omega a_x, \qquad a_x^2 = \omega a_x^1, \ldots$$
$$a_y^1 = \omega a_y, \qquad a_y^2 = \omega a_y^1, \ldots \tag{9}$$

with the assumption

$$|\omega| = \left|\frac{a^{i+1}}{a^i}\right| \ll 1 \tag{10}$$

By augmenting the dynamics of these new states to Eq. (2), an approximate dynamical model that includes this new target model is truncated as

$$\begin{bmatrix} \mathrm{d}a_x \\ \mathrm{d}a_y \\ \mathrm{d}a_x^1 \\ \mathrm{d}a_y^1 \\ \cdot \\ \cdot \\ \mathrm{d}a_x^i \\ \mathrm{d}a_y^i \end{bmatrix} = \begin{bmatrix} -\frac{\Theta}{2} & 0 & 0 & -1 & 0 & 0 \\ & -\frac{\Theta}{2} & 1 & 0 & 0 & 0 \\ & & -\frac{\Theta}{2} & 0 & 0 & -1 \\ & & & -\frac{\Theta}{2} & 1 & 0 \\ & \text{zero} & & & -\frac{\Theta}{2} & 0 \\ & \text{elements} & & & & -\frac{\Theta}{2} \end{bmatrix} \times \begin{bmatrix} a_x \\ a_y \\ a_x^1 \\ a_y^1 \\ \cdot \\ \cdot \\ a_x^i \\ a_y^i \end{bmatrix} + \begin{bmatrix} -a_y \\ a_x \\ -a_y^1 \\ a_x^1 \\ \cdot \\ \cdot \\ -a_y^i \\ a_x^i \end{bmatrix} \mathrm{d}\theta \tag{11}$$

Note that ω does not appear explicitly in Eq. (11), and Eq. (11) is a linear stochastic differential equation. An idea of this sort, given in Ref. 10 for a scalar problem, led to significantly improved filter performance.

B. Two-Dimensional Intercept

The two-dimensional intercept problem is developed in a relative inertial coordinate system. The system dynamics are expressed in the following set of equations:

$$\dot{x}_r = u_r, \qquad \dot{y}_r = v_r$$

$$\dot{u}_r = a_{T_{x_r}} - a_{M_{x_r}}, \qquad \dot{v}_r = a_{T_{y_r}} - a_{M_{y_r}}$$

$$a_{T_{x_r}} = a_T \cos(\omega t + \theta), \qquad a_{T_{y_r}} = a_T \sin(\omega t + \theta) \tag{12}$$

With the assumption of $\omega \ll 1$ and truncation of the target dynamics up to the second order, the 10-element state vector is defined as

$$x \equiv \left[x_r \;\; y_r \;\; u_r \;\; v_r \;\; a_x \;\; a_y \;\; a_x^1 \;\; a_y^1 \;\; a_x^2 \;\; a_y^2\right]^T$$

$$= \left[x_1 \;\; x_2 \;\; x_3 \;\; x_4 \;\; x_5 \;\; x_6 \;\; x_7 \;\; x_8 \;\; x_9 \;\; x_{10}\right]^T \tag{13}$$

Thus, in terms of the expanded state space, the linear, stochastic state differential equation is described by

$$dx = (Fx + Bu)\,dt + G\,d\theta \tag{14}$$

where F is given by the relations in Eqs. (12) and by the coefficient matrix of x in Eq. (11) where $i = 2$, B is a 10×2 matrix of zeros except for $B_{31} = B_{42} = -1$, $u = (a_{M_{x_r}}, a_{M_{y_r}})^T$, and

$$G = \left[0 \;\; 0 \;\; 0 \;\; 0 \;\; -x_6 \;\; x_5 \;\; -x_8 \;\; x_7 \;\; -x_{10} \;\; x_9\right]^T \tag{15}$$

C. Measurement

Angle Measurement

Angle information in discrete time is assumed. Then, the measurement at time t_k is

$$z_1(t_k) = h_1\left[x(t_k)\right] + v_k = \tan^{-1}(y_r/x_r) + v_k \triangleq z^*(t_k) + v_k \tag{16}$$

where v_k is a white random sequence with statistics

$$E[v_k] = 0, \qquad E[v_k v_l^T] = V_1 \delta_{kl} \tag{17}$$

Fictitious Measurement

In Refs. 7 and 8 the filter performance is improved by introducing a kinematic constraint based on a priori knowledge, which is implemented in the form of an augmented fictitious measurement. In particular, the acceleration vector is assumed to be related to the velocity as

$$V_T \cdot a_T = 0 \tag{18}$$

under the assumption that the target accelerates predominantly orthogonally to its velocity vector. When this condition is not met, the acceleration has a component in the direction of the target velocity as

$$V_T \cdot a_T = \eta \tag{19}$$

where V_T and a_T are assumed to be random vectors representing target velocity and acceleration, and η is the uncertainty in the orthogonality. This idea can be implemented in the form of a discrete pseudomeasuremnt as

$$z_2(t_k) = h_2\left[x(t_k)\right] + \eta_k$$

$$= V_{T_{x_r}} a_{T_{x_r}} + V_{T_{y_r}} a_{T_{y_r}} + \eta_k \tag{20}$$

where η_k is a white random sequence with assumed statistics

$$E[\eta_k] = 0, \qquad E[\eta_k \eta_l^T] = V_2 \delta_{kl} \tag{21}$$

Note that the variance of the measurement noise corresponds to the tightness of the constraint. In other words, the larger the variance, the more relaxed are the requirements on the longitudinal acceleration. This fictitious measurement is used along with the angle measurement in the modified-gain extended Kalman filter described in the next section.

IV. Estimation of Target States

In this section, the modified-gain extended Kalman filter (MGEKF)[11] is derived for the circular target model and for the fictitious and angle measurements defined in the previous section. Also considered is the method to reconstruct the maneuver rate using the estimated states. Given the continuous-time dynamics and discrete-time measurements, as in the previous section, construction of the filter is completed by specifying the time propagation and measurement update procedures.

A. Time Propagation

The state estimate $\bar{x}(t/t_{i-1})$ is propagated from the current time t_{i-1} to the next sample time t_i by integrating

$$\dot{\bar{x}}(t/t_{i-1}) = F\bar{x}(t/t_{i-1}) + Bu(t)$$

$$\dot{\bar{P}}(t/t_{i-1}) = F\bar{P}(t/t_{i-1}) + \bar{P}(t/t_{i-1})F^T + E[G\Theta G^T]$$

$$\dot{X}(t) = FX(t) + X(t)F^T + E[G\Theta G^T] \tag{22}$$

given the posteriori estimate $\bar{x}(t_{i-1}/t_{i-1}) = \hat{x}(t_{i-1})$ and posteriori pseudoerror variance $\bar{P}(t_{i-1}/t_{i-1}) = P(t_{i-1})$. The notation $R(t/t_{i-1})$ denotes the value of some quantity R at time t given the measurement sequence up to time t_{i-1}. The integration of the covariance of the state $X(t)$ begins with $X(0)$ at time $t = 0$. Upon integrating the foregoing equations to the next sample time, the propagated estimates are obtained as follows:

$$\bar{x}(t_i) = \bar{x}(t_i/t_{i-1}), \qquad \bar{P}(t_i) = \bar{P}(t_i/t_{i-1}) \tag{23}$$

It should be noted that since the process noise is state-dependent, the integration to propagate $\bar{P}(t)$ also requires the integration of $\dot{X}(t)$, where the $E[G\Theta G^T]$ matrix turns out to have nonzero elements for its lower-right 6×6 matrix. Note that the approximation technique reduces the originally nonlinear dynamics to linear dynamics. This allows for the closed-form solutions of the propagation of the estimates rather than performing online integration.

B. Measurement Update[11]

The states are updated as follows:

$$\hat{x}(t_i) = \bar{x}(t_i) + K(t_i)\left\{z - h\left[\bar{x}(t_i)\right]\right\}$$

$$K(t_i) = \bar{P}(t_i)H(t_i)^T\left[H(t_i)\bar{P}(t_i)H^T(t_i) + V\right]^{-1} \tag{24}$$

where

$$V = \begin{bmatrix} V_1 & 0 \\ 0 & V_2 \end{bmatrix}$$

and

$$\left.\frac{\partial h}{\partial x}\right|_{x(t_i)=\bar{x}(t_i)} \triangleq H(t_i)$$

$$= \begin{bmatrix} H_{11}, & H_{12}, & 0, & 0, & 0, & \ldots, & \ldots, & 0 \\ 0, & 0, & H_{23}, & H_{24}, & H_{25}, & H_{26}, & \ldots, & 0 \end{bmatrix} \tag{25}$$

with

$$H_{11} = -\frac{\bar{y}_r}{\bar{x}_r^2 + \bar{y}_r^2}, \quad H_{12} = \frac{\bar{x}_r}{\bar{x}_r^2 + \bar{y}_r^2}$$

$$H_{23} = \bar{x}_5, \quad H_{24} = \bar{x}_6, \quad H_{25} = \bar{x}_3 + V_{x_M}, \quad H_{26} = \bar{x}_4 + V_{y_M}$$

where the missile acceleration in the x and y directions, a_{M_x} and a_{M_y} are assumed to be measured very accurately with onboard sensors.

The measurement update of the pseudoerror variance is performed by

$$P(t_i) = \left\{I - K(t_i)g\left[z(t_i), \bar{x}(t_i)\right]\right\}\bar{P}(t_i)\left\{I - K(t_i) \times g\left[z(t_i), \bar{x}(t_i)\right]\right\}^T + K(t_i)V(t_i)K(t_i)^T \tag{26}$$

where $g[z(t_i), \bar{x}(t_i)]$ is used in the update of P rather than H of Eq. (25) and is given as

$$h\left[x(t_i)\right] - h\left[\bar{x}(t_i)\right] = \begin{Bmatrix} \tan^{-1}\dfrac{y_r(t_i)}{x_r(t_i)} - \tan^{-1}\dfrac{\bar{y}_r(t_i)}{\bar{x}_r(t_i)} \\ h_2\left[x(t_i)\right] - h_2\left[\bar{x}(t_i)\right] \end{Bmatrix} = g\left[z(t_i), \bar{x}(t_i)\right]\left[x(t_i) - \bar{x}(t_i)\right] \tag{27}$$

Note that g is a 2×10 matrix of function explicit only in the known quantities z and $\bar{x}$. In this sense, the function h has a universal linearization with respect to the measurement function z. Unfortunately, this type of linearization with respect to the measurements occurs for only a few functions. It is applicable to angle measurements,[11] but not for our new pseudomeasurement. Therefore, we must for the pseudomeasurement revert back to the extended Kalman filter form and define

$$g_2\left[z(t_i), \bar{x}(t_i)\right]\left[x(t_i) - \bar{x}(t_i)\right] = h_2\left[x(t_i)\right] - h_2\left[\bar{x}(t_i)\right] = \frac{\partial h_2}{\partial x(t_i)}\bigg|_{x=\bar{x}}\left[x(t_i) - \bar{x}(t_i)\right] \tag{28}$$

where the expression for $\partial h_2/\partial x(t_i)|_{x=\bar{x}}$ is found in the second row of H in Eq. (25).

For angle measurements,[11]

$$h_1\left[x(t_i)\right] - h_1\left[\bar{x}(t_i)\right] = g_1\left[z(t_i), \bar{x}(t_i)\right]\left[x(t_i) - \bar{x}(t_i)\right] = -E(t_i)\bar{H}\left[z^*(t_i)\right]\left[x(t_i) - \bar{x}(t_i)\right] \tag{29}$$

where

$$E(t_i) = \frac{D(t_i)\tan^{-1}\alpha(t_i)}{\alpha(t_i)}$$

$$D(t_i) = \frac{\sqrt{x_r(t_i)^2 + y_r(t_i)^2}}{\left[x_r(t_i)\bar{x}_r(t_i) + y_r(t_i)\bar{y}_r(t_i)\right]}$$

$$\alpha(t_i) = D(t_i)\bar{H}\left[z^*(t_i)\right]\bar{x}(t_i)$$

$$\bar{H}\left[z^*(t_i)\right] = \left[\sin z^*(t_i), \ -\cos z^*(t_i), \ 0, \ 0, \ 0, \ \ldots\right] \tag{30}$$

As discussed in Ref. 11, $g[z(t_i), \bar{x}(t_i)]$ is only used in the update of $P(t_i)$ but not in the gain, since it was empirically shown that this procedure leads to an unbiased estimate of the state.

C. Estimation of ω and T_{go}

Since the target angular velocity term is embedded in the states, ω should be reconstructed using the estimated states. A simple way to determine the value of ω is to divide the states as $\omega = a_x^1/a_x$ or a_x^2/a_x^1. However, since the expanded state space is originally an approximated state space, this might lead to numerical errors, especially when the higher approximated terms are used. By relying on the definition of the vector relation between velocity and acceleration, the target angular velocity can be obtained without using the augmented states. From the assumed dynamics, the target angular velocity during its evasive maneuver is

$$\omega_T = \frac{V_T \times a_T}{|V_T|^2} \tag{31}$$

Thus, by using the state estimates, ω is constructed as

$$\hat{\omega} = \text{sign}\left(\hat{V}_{T_x}\hat{a}_{T_y} - \hat{V}_{T_y}\hat{a}_{T_x}\right)\left|\frac{\hat{a}_T}{\hat{V}_T}\right| \tag{32}$$

To be used later in the controller, an estimate of time to go, T_{go}, is required, and approximated here as

$$\hat{T}_{go} = \frac{\hat{R}}{|\hat{\dot{R}}|} = \frac{\hat{R}}{|\hat{X}\cdot\hat{V}|/\hat{R}} \tag{33}$$

where $\hat{R}$ and $\hat{\dot{R}}$ are the estimates of relative range and range rate, respectively, and the vectors $\hat{X}$ and $\hat{V}$ are the estimates of relative position and velocity, respectively.

V. Linear Quadratic Guidance Law

Based on the estimated states and the estimate of the rotation rate constructed from the estimated states, a guidance law can be mechanized. In the following pages, a stochastic guidance law is determined that minimizes a quadratic performance index subject to the stochastic engagement dynamics, including the stochastic circular target model (8) under the assumption that states including the target states and target rotation rate are known perfectly. This assumption simplifies the derivation of the guidance law enormously, and for this homing problem it is shown that the solution to the stochastic control problem with state-dependent noise can be obtained in closed form. The solution obtained does not produce a certainty equivalence controller since the guidance law explicitly depends on the system statistics.

Note that since the noise in each Cartesian direction is correlated in the stochastic circular target model (8), and that with a_{T_x} and a_{T_y} dynamically coupled through the ω term, the guidance commands in the x and y direction cannot be achieved independently. Thus, the optimal stochastic controller for a circular target model is based on the minimization of the performance index

$$J = E\left[\frac{1}{2}\left(x_f^2 + y_f^2\right) + \frac{c}{2}\int_0^{t_f}\left(a_{M_x}^2 + a_{M_y}^2\right)\mathrm{d}t\right] \tag{34}$$

subject to the following stochastic system of linear dynamic equations:

$$\begin{aligned} \mathrm{d}x &= u\,\mathrm{d}t \\ \mathrm{d}y &= v\,\mathrm{d}t \\ \mathrm{d}u &= (a_{T_x} - a_{M_x})\,\mathrm{d}t \\ \mathrm{d}v &= (a_{T_y} - a_{M_y})\,\mathrm{d}t \\ \mathrm{d}a_{T_x} &= \left(-\frac{\Theta}{2}a_{T_x} - \omega a_{T_y}\right)\mathrm{d}t - a_{T_y}\,\mathrm{d}\theta \\ \mathrm{d}a_{T_y} &= \left(-\frac{\Theta}{2}a_{T_y} + \omega a_{T_x}\right)\mathrm{d}t + a_{T_x}\,\mathrm{d}\theta \end{aligned} \tag{35}$$

where θ is a Brownian motion defined earlier and $E[\cdot]$ denotes

an expectation operator. In the construction of the filter, the inherent nonlinearity of the target model was removed by an expansion of state variables. However, for the guidance law formulation, the rotation rate ω is assumed known, although it must be constructed online from the state estimator (32).

For brevity of notation, define the state and control vectors as follows:

$$x \triangleq \left[x,\ y,\ u,\ v,\ a_{T_x},\ a_{T_y}\right]^T$$
$$u \triangleq \left[a_{M_x},\ a_{M_y}\right]^T \tag{36}$$

Then, the stochastic control problem is to find u that minimizes

$$J = E\left[\frac{1}{2}\int_0^{t_f} u^T R u\ d\tau + \frac{1}{2}x_f^T S_f x_f\right] \tag{37}$$

subject to the stochastic differential equation with state-dependent noise

$$dx = (Ax + Bu)\,dt + D(x)\,d\theta \tag{38}$$

where

$$A = \begin{bmatrix} 0 & 0 & 1 & 0 & 0 & 0 \\ 0 & 0 & 0 & 1 & 0 & 0 \\ 0 & 0 & 0 & 0 & 1 & 0 \\ 0 & 0 & 0 & 0 & 0 & 1 \\ 0 & 0 & 0 & 0 & -\frac{\Theta}{2} & -\omega \\ 0 & 0 & 0 & 0 & \omega & -\frac{\Theta}{2} \end{bmatrix}, \quad B = \begin{bmatrix} 0 & 0 \\ 0 & 0 \\ 1 & 0 \\ 0 & 1 \\ 0 & 0 \\ 0 & 0 \end{bmatrix} \tag{39}$$

$$D(x) = \begin{bmatrix} 0 \\ 0 \\ 0 \\ 0 \\ -x_6 \\ x_5 \end{bmatrix}, \quad R = c\begin{bmatrix} 1 & 0 \\ 0 & 1 \end{bmatrix}$$

$$S_f = \begin{bmatrix} 1 & 0 & 0 & 0 & 0 & 0 \\ & 1 & 0 & 0 & 0 & 0 \\ & & 0 & 0 & 0 & 0 \\ & & & 0 & 0 & 0 \\ & & & & 0 & 0 \\ & & & & & 0 \end{bmatrix}$$

where $c > 0$. Note that

$$D(x) = \sum_{j=1}^{6} x_j D_j, \qquad D_j \in R^{6\times 1} \tag{40}$$

where x_j is the jth element of x and where

$$D_1, D_2, D_3, D_4 = \begin{bmatrix} 0 \\ 0 \\ 0 \\ 0 \\ 0 \\ 0 \end{bmatrix}, \quad D_5 = \begin{bmatrix} 0 \\ 0 \\ 0 \\ 0 \\ 0 \\ 1 \end{bmatrix}, \quad D_6 = \begin{bmatrix} 0 \\ 0 \\ 0 \\ 0 \\ -1 \\ 0 \end{bmatrix} \tag{41}$$

To obtain an optimal control for this class of problem, dynamic programming[13,14] is employed whereby the Hamilton-Jacobi-Bellman equation becomes

$$0 = J_t^o(x,t) + \min_u \left\{J_x^o(Ax + Bu) + \frac{1}{2}\left[x^T\Delta(J_{xx}^o, t)x + u^T R u\right]\right\} \tag{42}$$

where J^o is the optimal return function and the subscripts denote partial derivatives. The elements of the matrix Δ for any symmetric matrix W are defined as

$$\Delta_{ij}(W,t) = \mathrm{tr}\left[D_i(t)^T W D_j(t)\right] \tag{43}$$

The minimization operator in Eq. (25) produces

$$u = -R^{-1}B^T J_x^o \tag{44}$$

By substituting Eq. (44) into Eq. (42), the dynamic programming equation becomes

$$0 = J_t^o + J_x^o Ax - \frac{1}{2}J_x^o B R^{-1} B J_x^o + \frac{1}{2}x^T\Delta(J_{xx}^o, \Theta, t)x \tag{45}$$

The optimization problem is solved by explicitly showing that the foregoing equation has a solution. Assume $J^o(x,t) = \frac{1}{2}x^T S(t)x$; then

$$J_t^o = \frac{1}{2}x^T\dot{S}x, \qquad J_x^o = x^T S, \qquad J_{xx}^o = S \tag{46}$$

With this assumption, the dynamic programming equation is satisfied for all $x \in R^n$ if

$$\dot{S} + SA + A^T S + \Delta - SBR^{-1}B^T S = 0, \qquad S(t_f) = S_f \tag{47}$$

The desired optimal controller becomes

$$u = -R^{-1}B^T S x \tag{48}$$

where S is the solution of the Riccati equation, and $\Delta(S,t)_{ij} = \mathrm{tr}(D_i^T S D_j)$ leads to

$$\Delta = \begin{bmatrix} \text{zero} \\ \text{elements} & & \\ & S_{66} & -S_{56} \\ & -S_{56} & S_{55} \end{bmatrix} \tag{49}$$

The fact that Δ has only nonzero elements for its lower-right 2×2 matrix allows a tractable closed-form solution. To see the characteristics of the solution in a simple manner, matrices are partitioned such that their lower-right block partitioned is a 2×2 matrix. Then,

$$A = \begin{bmatrix} A_{11} & A_{12} \\ 0 & A_{22} \end{bmatrix}, \quad B = \begin{bmatrix} B_1 \\ 0 \end{bmatrix}$$
$$S = \begin{bmatrix} S_{11} & S_{12} \\ S_{12}^T & S_{22} \end{bmatrix}, \quad \Delta = \begin{bmatrix} 0 & 0 \\ 0 & \tilde{S} \end{bmatrix} \tag{50}$$

where $\tilde{S}$ is the nonzero element block in Eq. (49). This leads to the controller

$$u = \begin{bmatrix} a_{M_x} \\ a_{M_y} \end{bmatrix} = -\frac{1}{c}\begin{bmatrix} B_1 S_{11} \\ B_2 S_{12} \end{bmatrix} x \tag{51}$$

where block matrices satisfy the decomposed Riccati equation

$$-\dot{S}_{11} = S_{11}A_{11} + A_{11}^T S_{11} - S_{11}B_1 R^{-1}B_1^T S_{11}$$
$$-\dot{S}_{12} = S_{11}A_{12} + S_{12}A_{22} + A_{11}^T S_{12} - S_{11}B_1 R^{-1}B_1^T S_{12}$$
$$-\dot{S}_{22} = S_{12}A_{12} + S_{22}A_{22} + A_{22}^T S_{22} + A_{12}^T S_{22} + \tilde{S} - S_{12}B_1 R^{-1}B_1^T S_{12} \tag{52}$$

Since the S_{22} block does not affect the block matrices S_{11} and S_{12}, the optimal control law is not dependent on S_{22}. Therefore, the closed-form optimal guidance law for this special class of problems can be obtained by integrating the Riccati equation backwards without requiring the explicit evaluation of the Δ term. In particular, the stochastic optimal control problem essentially degenerates to a deterministic optimal control problem although the Itô terms are retained. The solution process for this deterministic control problem, explained in detail in Appendix A, produces a guidance law in closed form. Note that the deterministic coefficient A_{22} includes the statistic Θ. Therefore, the resulting controller is not a certainty equivalence controller. The new controller becomes

$$\begin{bmatrix} a_{M_x} \\ a_{M_y} \end{bmatrix} = \begin{bmatrix} c_1 & 0 & c_2 & 0 & c_3 & c_4 \\ 0 & c_1 & 0 & c_2 & -c_4 & c_3 \end{bmatrix} \begin{bmatrix} x(t) \\ y(t) \\ u(t) \\ v(t) \\ a_{T_x}(t) \\ a_{T_y}(t) \end{bmatrix} \tag{53}$$

where the gains c_1 to c_4 are an explicit function of T_{go}, ω, and Θ as

$$c_1 = \frac{T_{go}}{c + (T_{go}^3/3)}$$

$$c_2 = \frac{T_{go}^2}{c + (T_{go}^3/3)}$$

$$c_3 = c^* \left\{ \frac{\Theta T_{go}}{2} e^{(\Theta/2)T_{go}} - \sin\omega T_{go} \frac{\omega\Theta}{[(\Theta^2/4)+\omega^2]} + \left[\cos\omega T_{go} - e^{(\Theta/2)T_{go}}\right] \frac{[(\Theta^2/4)-\omega^2]}{[(\Theta^2/4)+\omega^2]} \right\}$$

$$c_4 = c^* \left\{ -\omega T_{go} e^{(\Theta/2)T_{go}} + \left[e^{(\Theta/2)T_{go}} - \cos\omega T_{go}\right] \frac{\omega\Theta}{[(\Theta/4)+\omega^2]} - \sin\omega T_{go} \frac{[(\Theta^2/4)-\omega^2]}{[(\Theta^2/4)+\omega^2]} \right\} \tag{54}$$

where

$$c^* = \frac{T_{go}}{e^{(\Theta/2)T_{go}}\left[c + (T_{go}^3/3)\right]\left[(\Theta^2/4)+\omega^2\right]}$$

Figure 2 is a block diagram for an adaptive guidance scheme for a homing missile. Note that guidance gains are functions of $\hat{T}_{go}$, estimated time to go, the statistic Θ, and the estimated maneuver rate $\hat{\omega}$. Therefore, for the bearing-only measurement system, although the resulting stochastic guidance law is suboptimal since the measurements are nonlinear functions of the states, the explicit dependence on the estimate of the target maneuver rate is a new feature that should help reduce terminal miss distance.

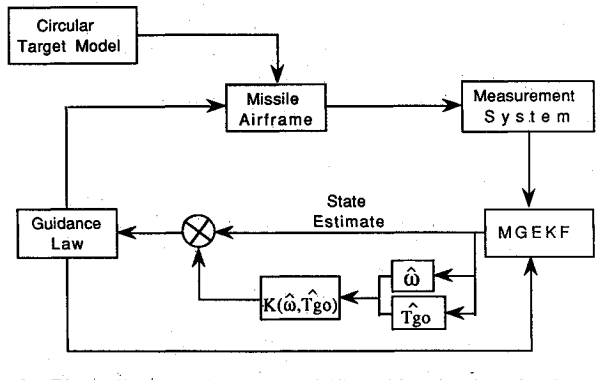

Fig. 2 Block diagram of homing missile guidance using circular target maneuver model.

VI. Numerical Simulation

For a particular engagement scenario, the performance of the estimator using the new target models and that of the guidance law are evaluated.

A. Missile and Target Model

Both the target and missile are treated as point masses and are considered in two-dimensional reference frames as shown in Fig. 1. The missile represents a highly maneuverable, short-range, air-to-air missile with a maximum normal acceleration of 100 g. It is launched with a velocity $M=0.9$ at a 10,000 ft altitude with zero normal acceleration. After a 0.4 s delay to clear the launch rail, it flies by the guidance command provided by the linear quadratic guidance law of Sec. V. Also, to compensate for the aerodynamic drag and propulsion, the missile is modeled to have a known longitudinal acceleration profile: $a_M = 25\ g$ for $t \le 2.6$ s, $a_M = -15\ g$ for $t > 2.6$ s. The target model flies at a constant speed of $M=0.9$ and at an altitude of 10,000 ft. It accelerates at 9 g either at the beginning or in the middle of the engagement. Thus, the rotation rate of the target is 0.3 during its maneuver.

Two engagements considered in the following section are shown in Fig. 3. With R_i and R_M denoting initial range and maneuver onset range, respectively, engagement 1 represents the situation in which the target maneuver starts at the beginning, and for engagement 2 the maneuver starts in the middle.

B. Filter Parameters and Initial Conditions

The integration of actual trajectories is performed by a fourth-order Runge-Kutta integrator with a step size of 0.02 s. The variance for the angle measurement is chosen, as given in Ref. 4, to be

$$V_1 = aV_0, \qquad V_0 = \frac{\left[(0.25/R^2) + 5.625\times 10^{-7}\right]}{\Delta t}\ \text{rad}^2 \tag{55}$$

where R is the range, Δt the filter sample time, and a the parameter used in the simulation indicating different levels of sensor accuracy.

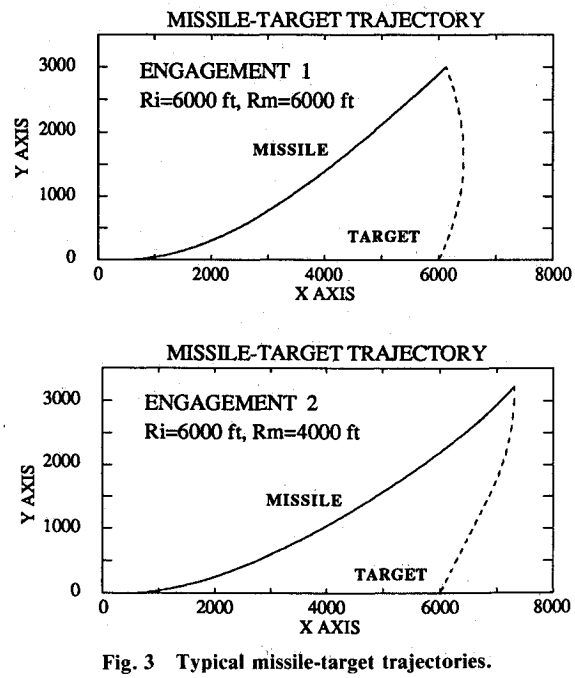

Fig. 3 Typical missile-target trajectories.

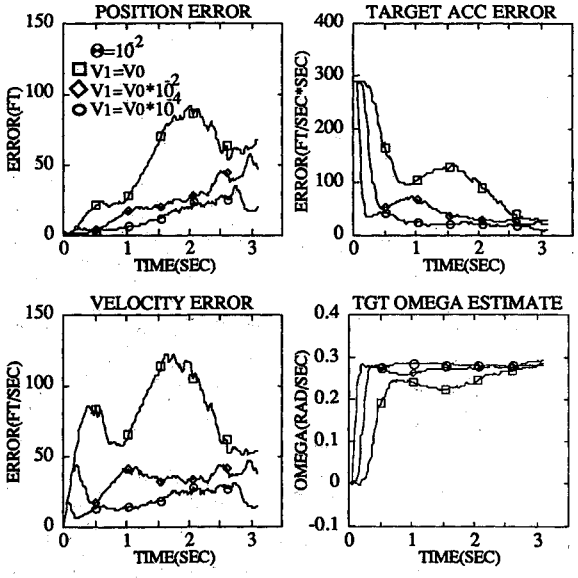

Fig. 4 Circular target model with different V_1 (engagement 1).

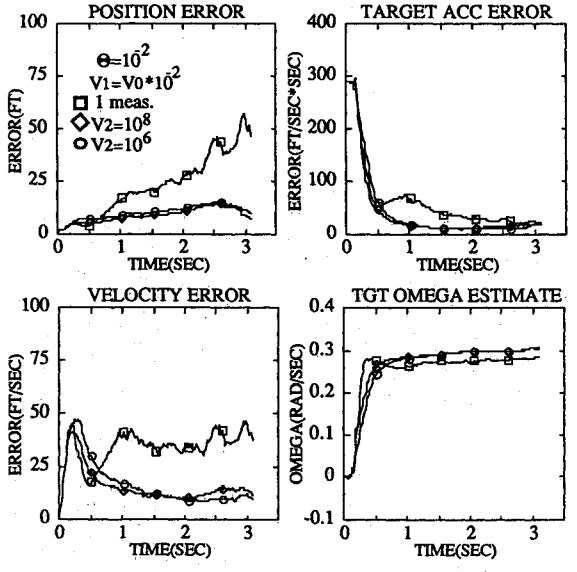

Fig. 5 Circular target model with pseudomeasurement (engagement 1).

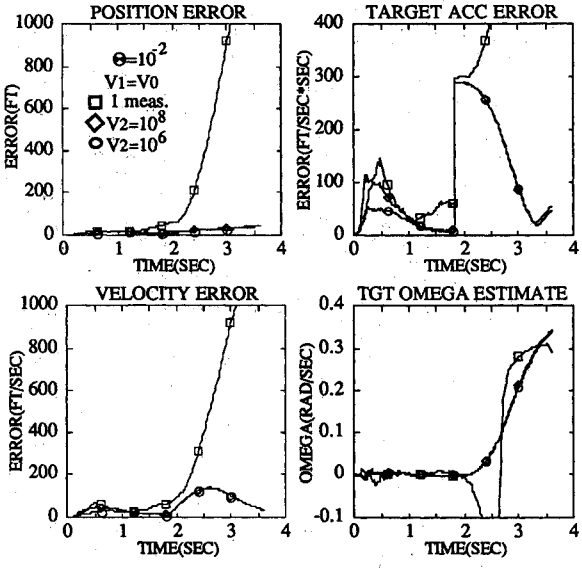

Fig. 6 Circular target model with pseudomeasurement (engagement 2).

As mentioned earlier, the variance for the pseudomeasurement can be interpreted to show how strictly the orthogonality assumption between the target velocity and acceleration is to be kept. By allowing some acceleration in the longitudinal direction, a reasonable estimate of the variance to be used can be given. Suppose that the acceleration component in the velocity direction has a normal distribution with a zero mean. Then with probability 0.95, a 1-g acceleration while flying with $V_T = 970$ ft/s leads to $2\sigma = 3.12 \times 10^4$ (ft^2/s^3), where σ is the standard deviation, which results in a variance $V_2 = 2.44 \times 10^8$ (ft^2/s^3)^2.

Unless otherwise stated, the filter is initialized at launch with the true relative position and relative velocity component values assumed obtained from the launch aircraft. Hence, the initial values for the diagonal elements of the covariance matrix associated with position and velocity, P_{11}, P_{22}, P_{33}, and P_{44}, are set to 10, and this ensures positive definiteness. On the other hand, little knowledge about target acceleration is assumed to be provided at the beginning. Therefore, the initial values for the target acceleration and expanded states are zero. The initial values of the covariance matrix associated with target acceleration are calculated by resorting to the definition of the target acceleration at $t = 0$ given in Eq. (2). These covariances are presented in Appendix B. The target is expected to execute a maximum acceleration turn in its evasive motion, and the missile has no knowledge about the direction of target rotation. Note that θ is a Brownian motion process beginning at $\theta(0) = \bar{\theta}$, the expected angle the target acceleration vector makes with respect to the x_r axis at the time of launch, and $a_{T_{\max}}$ is the expected maximum acceleration of the target. For the simulation with a coordinate system having one axis perpendicular to the initial V_T direction, $\bar{\theta}$ is zero. Then, the possible nonzero elements of the upper triangular part of the initial covariance are $P_{55}(0)$, $P_{57}(0)$, $P_{59}(0)$, $P_{77}(0)$, $P_{79}(0)$, and $P_{99}(0)$. Furthermore, no information is available about the direction of the maneuver, and the possible maximum rotation rate can be either positive or negative. Thus, the odd powers of $\bar{\omega}$ are taken as zero. This leaves only $P_{55}(0)$, $P_{59}(0)$, $P_{77}(0)$, and $P_{99}(0)$ as the nonzero elements. However, a value of 10 is assigned to P_{66}, P_{88}, and P_{1010} to ensure the positive definiteness of the covariance matrix at the initial time.

C. Filter Results

The results in this section are the product of a Monte Carlo analysis consisting of 50 filter runs. Along with the miss distance calculations, the plots of the estimation error and the ω estimates vs time are mainly considered. The errors are calculated as $[E[e_x]^2 + E[e_y]^2]^{1/2}$ where $E[e_x]$ and $E[e_y]$ are the averaged values of the error over 50 simulation runs. In evaluating the actual miss distances, the filter state estimates are used in the guidance law. Moreover, the tracking errors to be presented next are based on the guidance law in terms of the estimated states, since the tracking errors were observed to be quite similar to those in the case where the actual states are used for the guidance law.

Figure 4 displays the results for engagement 1 where the target maneuver is initiated at $t = 0$ and the pseudomeasurement is not used. It is shown that the estimation improves with better angle measurements.

When the auxiliary pseudomeasurement is also implemented in the filter, estimation performance improves over the case in which only an angle measurement is used. This is shown in Fig. 5, where again the target starts its acceleration maneuver at the beginning of the engagement ($R_i = R_M$). At first, the filter with the fictitious measurement seems to work a little worse than the filter with angle-only measurement. Then, the fictitious measurement promptly works as if it suppressed or delayed the filter divergence. Note that the effect of two values of pseudonoise variance is shown.

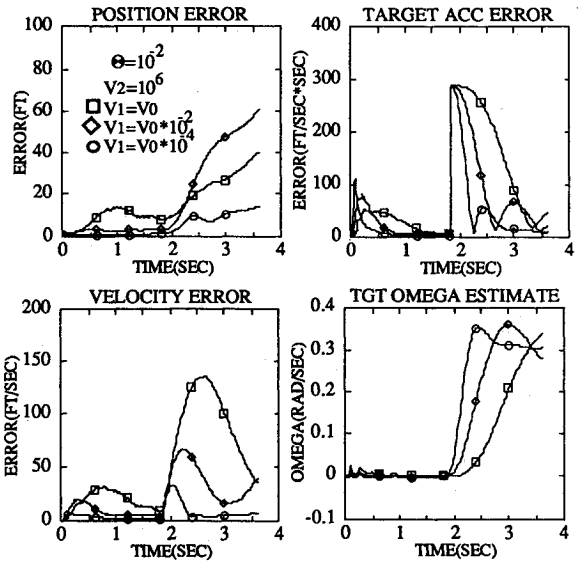

Fig. 7 Circular target model with pseudomeasurement (engagement 2).

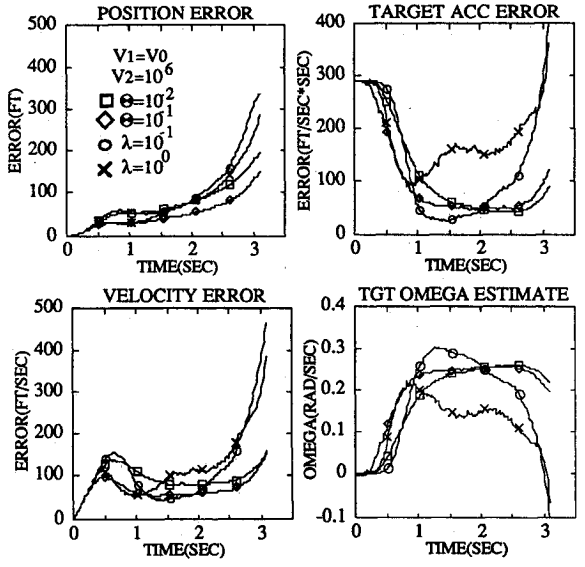

Fig. 8 Comparison with Gauss-Markov model (engagement 1).

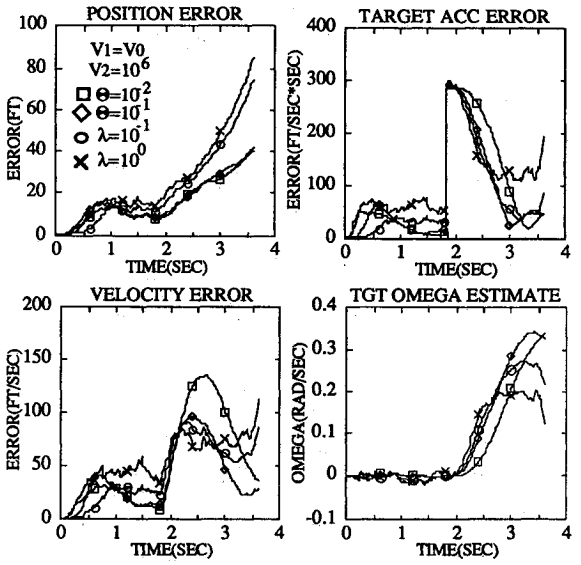

Fig. 9 Comparison with Gauss-Markov model (engagement 2).

Table 1 Comparison of miss distance

Statistic	Case	Range_i, ft	Range_M, ft	Miss distance, ft
$\lambda = 0.1$	I	6000	6000	0.57
$V_1 = V_0$		6000	4000	0.53
$V_2 = 10^6$	II	6000	6000	10.13
		6000	4000	73.08
	III	6000	6000	9.42
		6000	4000	5.08
$\lambda = 1.0$	II	6000	6000	8.14
$V_1 = V_0$		6000	4000	60.49
$V_2 = 10^6$	III	6000	6000	7.24
		6000	4000	2.30
$\Theta = 0.01$	I	6000	6000	0.35
$V_1 = V_0 \times 10^{-2}$		6000	4000	0.32
$V_2 = 10^6$	II	6000	6000	1.30
		6000	4000	0.74
	III	6000	6000	0.82
		6000	4000	0.54
$\Theta = 0.001$	II	6000	6000	2.65
$V_1 = V_0$		6000	4000	1.71
$V_2 = 10^6$	III	6000	6000	2.13
		6000	4000	1.36
$\Theta = 0.01$	II	6000	6000	4.59
$V_1 = V_0$		6000	4000	1.97
$V_2 = 10^6$	III	6000	6000	4.29
		6000	4000	1.82
$\Theta = 0.1$	II	6000	6000	4.98
$V_1 = V_0$		6000	4000	2.07
$V_2 = 10^6$	III	6000	6000	4.86
		6000	4000	2.01
$\Theta = 0.001$	II	6000	6000	2.65
$V_1 = V_0$		6000	4000	1.71
$V_2 = 10^8$	III	6000	6000	2.34
		6000	4000	1.49

The role of the fictitious measurement is more observable for engagement 2 where the target maneuver begins in the middle of the engagement ($R_M = 4000$ ft). As plotted in Fig. 6, the filter equipped with only the angle measurement diverges as soon as the target maneuver occurs. On the other hand, when the filter is augmented with the fictitious measurement, it works very effectively. The divergence of position and velocity is noticeably suppressed, and the acceleration estimate tends to return to its actual value from an instantaneous large acceleration error. With the accuracy of the angle measurement increased, the target acceleration estimate after the maneuver onset improves faster than the filter that uses poor angle measurements. This is shown in Fig. 7.

The performance of the current target models is also compared with that of the Gauss-Markov target model. The two models assume the same magnitude of target acceleration. Note that in a Gauss-Markov model,[3,4] λ, the target maneuver time constant, and W, the strength of the dynamic driving noise in the model, are two parameters but are varied relative to one another and they are essentially tuning parameters. However, the tuning parameter is Θ in the new target model. Along with the kinematic constraint incorporated as a pseudomeasurement, the modified-gain extended Kalman filter is built to estimate the target states, and the guidance law[4] is based on the Gauss-Markov target model. Figures 8 and 9 show how well the filter estimates the target states. Note that the circular target model estimates the target state better than the Gauss-Markov model. It was also observed through the simulation that the estimation performance of the Gauss-Markov target model has been improved with the pseudomeasurement, and this is reflected in the miss distance calculations to be presented. This is because the kinematic constraint increases the fidelity of the Gauss-Markov model.

Miss distances have been calculated on the basis of 50 runs of a Monte Carlo simulation with an approximate error of ± 0.02 ft due to subdiscretization near the final time. In the simulation that produces Table 1, the actual states are fed to the guidance law in case I, and the estimated states and maneuver rate estimate are fed to the guidance law in cases II and III. The estimates are obtained from angle-only measurements in case II, and from both an angle measurement and pseudomeasurement in case III.

Miss distance performance is tested as more noise is introduced into the measurement and then into the dynamics. Table 1 indicates that much improvement results with the circular target model, with additional improvements achieved through the kinematic constraint. In addition, miss distance has been improved by using the angle measurement and pseudomeasurement, especially as the process-noise power spectral density Θ in the state-dependent noise term decreases. The calculation of miss distance with the Gauss-Markov target model also indicates that significant improvement is obtained in the Gauss-Markov model using the kinematic constraint. For the particular scenario chosen here, a circular target model augmented by pseudomeasurement outperforms the Gauss-Markov target model.

VII. Conclusions

The orthogonality between the target acceleration and velocity vectors is a typical characteristic of the target of an air-to-air missile, and it is utilized in the development of a new stochastic target acceleration model for the homing missile problem. In addition, this characteristic is also implemented in the form of an augmented pseudomeasurement. A guidance law that minimizes a quadratic performance index subject to the stochastic engagement dynamics is determined in closed form where the gains are an explicit function of the estimated target maneuver rate and time to go. Preliminary results for the two-dimensional case indicate that the circular target model is able to produce a reliable estimate in the homing missile engagement. When it is augmented by the fictitious measurement, the modified-gain extended Kalman filter using the proposed target model results in the significant enhancement of target state estimation. The kinematic constraint also leads to significant improvement in miss distance performance for the Gauss-Markov target model. Comparisons of the current target models with the Gauss-Markov target model show that significant improvement is gained in both target state estimation and miss distance.

Appendix A: Linear Quadratic Guidance Law for Deterministic Circular Target Model

In the following, the optimal deterministic guidance law for a linear quadratic problem is sought for the current circular target model filter. The deterministic optimal solution can be obtained by solving the Riccati equation without the Δ term via the transition matrix approach, but the use of the Euler-Lagrange equation seems simpler for this case.

The problem is to minimize the performance index

$$J = \frac{1}{2}(x_f^2 + y_f^2) + \frac{c}{2}\int_t^{tf} (a_{M_x}^2 + a_{M_y}^2)\,dt \tag{A1}$$

subject to the following linear dynamic system:

$$\begin{aligned}
\dot{x} &= u \\
\dot{y} &= v \\
\dot{u} &= a_{T_x} - a_{M_x} \\
\dot{v} &= a_{T_y} - a_{M_y} \\
\dot{a}_{T_x} &= -\frac{\Theta}{2} a_{T_x} - \omega a_{T_y} \\
\dot{a}_{T_y} &= -\frac{\Theta}{2} a_{T_y} + \omega a_{T_x}
\end{aligned} \tag{A2}$$

This linear system of dynamics stems from taking the Itô derivative of the corresponding nonlinear stochastic target model (6). The ω is the angular rate of the target maneuver that is handled as a known constant in the derivations. In the actual mechanization of the guidance law, the value of $\hat{\omega}$ constructed from the estimated states is used.

The variational Hamiltonian and augmented end-point function are given by

$$\begin{aligned}
H &= ca_{M_x}^2 + ca_{M_y}^2 + \lambda_1 u + \lambda_2 v + \lambda_3(a_{T_x} - a_{M_x}) \\
&\quad + \lambda_4(a_{T_y} - a_{M_y}) + \lambda_5\left(-\frac{\Theta}{2} - \omega a_{T_y}\right) \\
&\quad + \lambda_6\left(-\frac{\Theta}{2} + \omega a_{T_x}\right)
\end{aligned} \tag{A3}$$

$$G = \frac{1}{2}(x_f^2 + y_f^2) \tag{A4}$$

where λ_i, $i = 1, \ldots, 6$ is a Lagrange multiplier. The Euler-Lagrange equations for λ_i are

$$\dot{\lambda}_1 = 0, \qquad \dot{\lambda}_2 = 0, \qquad -\dot{\lambda}_3 = \lambda_1, \qquad -\dot{\lambda}_4 = \lambda_2 \tag{A5}$$

where the optimal control satisfies the optimality condition

$$a_{M_x} = \frac{\lambda_3}{c}, \qquad a_{M_y} = \frac{\lambda_4}{c} \tag{A6}$$

Finally, the Euler-Lagrange equations with the natural boundary conditions yield

$$\lambda_1 = x_f, \qquad \lambda_2 = y_f, \qquad \lambda_3 = x_f T_{\text{go}}, \qquad \lambda_4 = y_f T_{\text{go}} \tag{A7}$$

which gives the control

$$a_{M_x} = x(t_f)T_{\text{go}}/c, \qquad a_{M_y} = y(t_f)T_{\text{go}}/c \tag{A8}$$

where T_{go} is the time to go of the missile to intercept the target, and c is the guidance law design parameter. In order to obtain the guidance law in terms of the current states, the underlining dynamics are integrated backward from t_f to t. The successive integrations of state differential equations yield

$$\begin{aligned}
a_{T_x} &= \cos\omega T_{\text{go}} e^{(\Theta/2)T_{\text{go}}} a_{T_x}(t_f) + \sin\omega T_{\text{go}} e^{(\Theta/2)T_{\text{go}}} a_{T_y}(t_f) \\
a_{T_y} &= -\sin\omega T_{\text{go}} e^{(\Theta/2)T_{\text{go}}} a_{T_x}(t_f) + \cos\omega T_{\text{go}} e^{(\Theta/2)T_{\text{go}}} a_{T_y}(t_f) \\
u &= \frac{1}{2c} T_{\text{go}}^2 x(t_f) + u(t_f) + \frac{1}{(\Theta^2/4) + \omega^2} \\
&\quad \times \left\{\frac{\Theta}{2}\left[1 - \cos\omega T_{\text{go}} e^{(\Theta/2)T_{\text{go}}}\right] - \omega \sin\omega T_{\text{go}} e^{(\Theta/2)T_{\text{go}}}\right\} \\
&\quad \times a_{T_x}(t_f) + \frac{1}{(\Theta^2/4) + \omega^2}\left\{-\omega\left[1 - \cos\omega T_{\text{go}} e^{(\Theta/2)T_{\text{go}}}\right]\right. \\
&\quad \left. - \frac{\Theta}{2}\sin\omega T_{\text{go}} e^{(\Theta/2)T_{\text{go}}}\right\} a_{T_y}(t_f) \\
v &= \frac{1}{2c} T_{\text{go}}^2 y(t_f) + v(t_f) + \frac{1}{(\Theta^2/4) + \omega^2} \\
&\quad \times \left\{\omega\left[1 - \cos\omega T_{\text{go}} e^{(\Theta/2)T_{\text{go}}}\right]\right. \\
&\quad \left. + \frac{\Theta}{2}\sin\omega T_{\text{go}} e^{(\Theta/2)T_{\text{go}}}\right\} a_{T_x}(t_f) + \frac{1}{(\Theta^2/4) + \omega^2} \\
&\quad \times \left\{\frac{\Theta}{2}\left[1 - \cos\omega T_{\text{go}} e^{(\Theta/2)T_{\text{go}}}\right]\right. \\
&\quad \left. - \omega \sin\omega T_{\text{go}} e^{(\Theta/2)T_{\text{go}}}\right\} a_{T_y}(t_f)
\end{aligned}$$

$$x = \left(1 - \frac{T_{go}^3}{6c}\right) x(t_f) - T_{go} u(t_f) + \frac{1}{(\Theta^2/4) + \omega^2}$$
$$\times \left\{ -\frac{\Theta T_{go}}{2} - \frac{[(\Theta^2/4) - \omega^2]}{[(\Theta^2/4) + \omega^2]} \left[1 - \cos\omega T_{go} e^{(\Theta/2)T_{go}}\right] \right.$$
$$\left. + \frac{\omega\Theta}{[(\Theta^2/4) + \omega^2]} \sin\omega T_{go} e^{(\Theta/2)T_{go}} \right\} a_{T_x}(t_f) + \frac{1}{(\Theta^2/4) + \omega^2}$$
$$\times \left\{ \omega T_{go} + \frac{\omega\Theta}{[(\Theta^2/4) + \omega^2]} \left[1 - \cos\omega T_{go} e^{(\Theta/2)T_{go}}\right] \right.$$
$$\left. + \frac{[(\Theta^2/4) - \omega^2]}{[(\Theta^2/4) + \omega^2]} \sin\omega T_{go} e^{(\Theta/2)T_{go}} \right\} a_{T_y}(t_f)$$
$$y = \left(1 - \frac{T_{go}^3}{6c}\right) y(t_f) - T_{go} v(t_f) + \frac{1}{(\Theta^2/4) + \omega^2}$$
$$\times \left\{ -\omega T_{go} - \frac{\omega\Theta}{[(\Theta^2/4) + \omega^2]} \left[1 - \cos\omega T_{go} e^{(\Theta/2)T_{go}}\right] \right.$$
$$\left. - \frac{[(\Theta^2/4) - \omega^2]}{[(\Theta^2/4) + \omega^2]} \sin\omega T_{go} e^{(\Theta/2)T_{go}} \right\} a_{T_x}(t_f) + \frac{1}{(\Theta^2/4) + \omega^2}$$
$$\times \left\{ -\frac{\Theta T_{go}}{2} - \frac{[(\Theta^2/4) - \omega^2]}{[(\Theta^2/4) + \omega^2]} \left[1 - \cos\omega T_{go} e^{(\Theta/2)T_{go}}\right] \right.$$
$$\left. + \frac{\omega\Theta}{[(\Theta^2/4) + \omega^2]} \sin\omega T_{go} e^{(\Theta/2)T_{go}} \right\} a_{T_y}(t_f) \qquad \text{(A9)}$$

With the final states being expressed in terms of the current states via a 6×6 matrix inversion, the optimal guidance law is obtained as Eq. (51). As expected from dynamic coupling in the target acceleration model, guidance commands in each channel are functions of the acceleration components in both the x and y directions.

Appendix B: State and Error Variance Associated with Target Acceleration

Since the initial values for the state estimates associated with target acceleration are set to zero, the state and error variances are computed with the aid of expected values of trigonometric functions such as

$$E[\cos^2\theta] = \int_{-\infty}^{+\infty} \cos^2\theta p(\theta)\, d\theta$$

with

$$p(\theta) = \frac{1}{\sqrt{2\pi\Theta t}} e^{-\left[\frac{(\theta - \bar{\theta})^2}{2\Theta t}\right]} \qquad \text{(B1)}$$

By using standard manipulation, the expected value of $\cos^2\theta$ is

$$E[\cos^2\theta] = \frac{1}{2}(1 + \cos 2\bar{\theta} e^{-2\Theta t}) \qquad \text{(B2)}$$

and in the same manner,

$$E[\sin^2\theta] = \frac{1}{2}(1 + \cos 2\bar{\theta} e^{-2\Theta t}) \qquad \text{(B3)}$$

$$E[\cos\theta \sin\theta] = \frac{1}{2} \sin 2\bar{\theta} e^{-2\Theta t} \qquad \text{(B4)}$$

This yields the initial conditions for the state and error variances associated with target acceleration as follows:

$$P_{55}(0) = X_{55}(0) = a_{T_{max}}^2 \times f1, \quad P_{56}(0) = X_{56}(0) = a_{T_{max}}^2 \times f2$$
$$P_{57}(0) = X_{57}(0) = a_{T_{max}}^2 \bar{\omega} \times f1, \quad P_{58}(0) = X_{58}(0) = a_{T_{max}}^2 \bar{\omega} \times f2$$
$$P_{59}(0) = X_{59}(0) = a_{T_{max}}^2 \bar{\omega}^2 \times f1, \quad P_{510}(0) = X_{510}(0) = a_{T_{max}}^2 \bar{\omega}^2 \times f2$$
$$P_{66}(0) = X_{66}(0) = a_{T_{max}}^2 \times f3, \quad P_{67}(0) = X_{67}(0) = a_{T_{max}}^2 \bar{\omega} \times f2$$
$$P_{68}(0) = X_{68}(0) = a_{T_{max}}^2 \bar{\omega} \times f3, \quad P_{69}(0) = X_{69}(0) = a_{T_{max}}^2 \bar{\omega}^2 \times f2$$
$$P_{610}(0) = X_{610}(0) = a_{T_{max}}^2 \bar{\omega}^2 \times f3, \quad P_{77}(0) = X_{77}(0) = a_{T_{max}}^2 \bar{\omega}^2 \times f1$$
$$P_{78}(0) = X_{78}(0) = a_{T_{max}}^2 \bar{\omega}^2 \times f2, \quad P_{79}(0) = X_{79}(0) = a_{T_{max}}^2 \bar{\omega}^3 \times f1$$
$$P_{710}(0) = X_{710}(0) = a_{T_{max}}^2 \bar{\omega}^3 \times f2, \quad P_{88}(0) = X_{88}(0) = a_{T_{max}}^2 \bar{\omega}^2 \times f3$$
$$P_{89}(0) = X_{89}(0) = a_{T_{max}}^2 \bar{\omega}^3 \times f2, \quad P_{810}(0) = X_{810}(0) = a_{T_{max}}^2 \bar{\omega}^3 \times f3$$
$$P_{99}(0) = X_{99}(0) = a_{T_{max}}^2 \bar{\omega}^4 \times f1, \quad P_{910}(0) = X_{910}(0) = a_{T_{max}}^2 \bar{\omega}^4 \times f2$$
$$P_{1010}(0) = X_{1010}(0) = a_{T_{max}}^2 \bar{\omega}^4 \times f3$$

where

$$f1 = \frac{(1 + \cos 2\bar{\theta})}{2}, \quad f2 = \frac{\sin 2\bar{\theta}}{2}, \quad f3 = \frac{(1 - \cos 2\bar{\theta})}{2}$$

Acknowledgment

This work was supported by the Air Force Armament Laboratory, Eglin Air Force Base, Florida, under Contract FO8635-87-K-0417.

References

[1]Chang, C. B., and Tabsczynsky, J. A., "Application of State Estimation to Target Tracking," *IEEE Transaction on Automatic Control*, Vol. AC-29, No. 2, 1984, pp. 98–109.

[2]Lin, C. F., and Shafroth, M. W., "A Comparative Evaluation of Some Maneuvering Target Tracking Algorithms," *Proceedings of the AIAA Guidance and Control Conference*, AIAA, New York, 1983, pp. 39–56.

[3]Vergez, P. L., and Liefer, R. K., "Target Acceleration Modeling for Tactical Missile Guidance," *Journal of Guidance, Control, and Dynamics*, Vol. 7, No. 3, 1984, pp. 315–321.

[4]Hull, D. G., Kite, P. C., and Speyer, J. L., "New Target Models for Homing Missile Guidance," *Proceedings of the AIAA Guidance and Control Conference*, AIAA, New York, 1983, pp. 22–29.

[5]Berg, R. F., "Estimation and Prediction for Maneuvering Target Trajectories," *IEEE Transaction on Automatic Control*, Vol. AC-28, No. 3, 1983, pp. 294–304.

[6]Song, T. L., Ahn, J. Y., and Park, C., "Suboptimal Filter Design with Pseudomeasurements for Target Tracking," *IEEE Transaction on Aerospace and Electronics*, Vol. 24, No. 1, 1988, pp. 28–39.

[7]Tahk, M. J., and Speyer, J. L., "Target Tracking Problems Subject to Kinematic Constraints," *Proceedings of 27th IEEE Conference on Decision and Control*, Inst. of Electrical and Electronics Engineers, New York, 1988, pp. 168–1059.

[8]Kim, K. D., Speyer, J. L., and Tahk, M., "Target Maneuver Models for Tracking Estimators," *Proceedings of the IEEE International Conference on Control and Applications*, Inst. of Electrical and Electronics Engineers, New York, 1989.

[9]Gustafson, D. E., and Speyer, J. L., "Linear Minimum Variance Filter Applied to Carrier Tracking," *IEEE Transaction on Automatic Control*, Vol. AC-21, No. 1, 1976, pp. 65–73.

[10]Speyer, J. L., and Gustafson, D. E., "An Approximation Method of Estimation in Linear Systems with Parameter Uncertainty," *IEEE Transaction on Automatic Control*, Vol. AC-20, No. 6, 1975, pp. 354–359.

[11]Song, T. L., and Speyer, J. L., "A Stochastic Analysis of a Modified Gain Extended Kalman Filter with Application to Estimation with Bearing Only Measurements," *IEEE Transaction on Automatic Control*, Vol. AC-30, No. 10, 1985, pp. 940–949.

[12]Jazwinski, A. H., *Stochastic Process and Filtering Theory*, Academic, New York, 1970.

[13]Wonham, W. M., "Random Differential Equations In Control Theory," *Probabilistic Methods in Applied Mathematics*, Vol. 2, Academic, New York, 1970.

[14]Bryson, A. E., and Ho, Y. C., *Applied Optimal Control Theory*, Wiley, New York, 1975.